Scientific Reports

https://doi.org/10.1038/s41598-026-37368-3

Article in Press

Enhancing red color performance in three-color electrophoretic displays using high-frequency voltage and low-voltage differential oscillation

Received: 20 June 2024

Accepted: 21 January 2026

Published online: 23 January 2026

Cite this article as: Jiang M., Yi Z., Wang J. *et al.* Enhancing red color performance in three-color electrophoretic displays using high-frequency voltage and low-voltage differential oscillation. *Sci Rep* (2026). https://doi.org/10.1038/s41598-026-37368-3

Mouhua Jiang, Zichuan Yi, Jiashuai Wang, Wanzhen Xu, Zhengxing Long, Li Wang, Liming Liu, Feng Chi, Ahmad Umar & Guofu Zhou

We are providing an unedited version of this manuscript to give early access to its findings. Before final publication, the manuscript will undergo further editing. Please note there may be errors present which affect the content, and all legal disclaimers apply.

If this paper is publishing under a Transparent Peer Review model then Peer Review reports will publish with the final article.

ARTICLE IN PRESS

© The Author(s) 2026. **Open Access** This article is licensed under a Creative Commons Attribution-NonCommercial-NoDerivatives 4.0 International License, which permits any non-commercial use, sharing, distribution and reproduction in any medium or format, as long as you give appropriate credit to the original author(s) and the source, provide a link to the Creative Commons licence, and indicate if you modified the licensed material. You do not have permission under this licence to share adapted material derived from this article or parts of it. The images or other third party material in this article are included in the article's Creative Commons licence, unless indicated otherwise in a credit line to the material. If material is not included in the article's Creative Commons licence and your intended use is not permitted by statutory regulation or exceeds the permitted use, you will need to obtain permission directly from the copyright holder. To view a copy of this licence, visit http://creativecommons.org/licenses/by-nc-nd/4.0/.

ARTICLE IN PRESS

Enhancing Red Color Performance in Three-Color Electrophoretic Displays Using High-Frequency Voltage and Low-Voltage Differential Oscillation

Mouhua Jiang [1,2], Zichuan Yi [1,*], Jiashuai Wang [1], Wanzhen Xu [1,2], Zhengxing Long [1,3], Li Wang [5], Liming Liu [1], Feng Chi [1] , Ahmad Umar[6,7,8,†], and Guofu Zhou [4]

[1] School of Electronic Information, University of Electronic Science and Technology of China, Zhongshan Institute, Zhongshan 528402, P.R. China.
[2] South China Academy of Advanced Optoelectronics, South China Normal University, Guangzhou 510006, China.
[3] School of Information and Optoelectronic Science and Engineering, South China Normal University, Guangzhou 510006, China.
[4] Guangdong Provincial Key Laboratory of Optical Information Materials and Technology, South China Academy of Advanced Optoelectronics, South China Normal University, Guangzhou 510006, P. R. China.
[5] School of Information Engineering, Zhongshan Polytechnic, Zhongshan 528400, China.
[6] Department of Chemistry, College of Science and Arts, Najran University, Najran-11001, Kingdom of Saudi Arabia
[7] STEM Pioneers Training Lab, Najran University, Najran-11001, Kingdom of Saudi Arabia
[8]Department of Materials Science and Engineering, The Ohio State University, Columbus, OH 43210, USA
[†] Adjunct Professor in the Department of Materials Science and Engineering, The Ohio State University, Columbus, OH 43210, USA

*Corresponding author. E-mail: yizichuan@zsc.edu.cn(Z.Y.);
Contributing authors: 2022024132@m.scnu.edu.cn (M.J.);
202221021120@std.uestc.edu.cn (J.W.);
2021024102@m.scnu.edu.cn (W.X.); mikaellzx@163.com

ARTICLE IN PRESS

ARTICLE IN PRESS

(Z.L.); creekxi@163.com (L.W.); liulmxps@126.com (L.L.);
chif-eng@semi.ac.cn (F.C.); umar.20@osu.edu (A.U.);
guofu.zhou@m.scnu.edu.cn (G.Z.)

Abstract

Three-color electrophoretic display (EPD) makes up for the limitation of traditional EPDs in color representation. However, when displaying red color, there are issues such as long response time and low red saturation. In order to improve these defects, a simulation model was constructed using COMSOL finite element simulation method to explore the movement of electro-phoretic particles. Leveraging the principles of three-color EPDs and electrophoresis theory, a novel driving scheme was proposed. This scheme employed high-frequency voltage and low-voltage differential oscillation, aiming to expedite the response time of red particles and enhance the red saturation. The final experimental results showed that the response time of the red particles was 1.76 s, a decrease of 2.42 s, the number of flickers was 1, a decrease of 8, and the maximum red saturation rose to 0.53, an increase of 0.08. The proposed driving scheme effectively improved the red display performance of three-color EPDs.

Keywords: three-color electrophoretic display, driving scheme, response time, high-frequency voltage

ARTICLE IN PRESS

1 Introduction

Three-color electrophoretic displays (EPDs), known for their reflective display technology, offer benefits including low energy consumption, visual health, and flexibility [1-3], Additionally, they effectively address the limitations of black and white EPDs in multi-color display performance. However, compared with traditional EPDs [4-6], three-color EPDs have a complex spatial distribution of particles due to the increase of particle types within microcapsules [7-9], resulting in a much longer response time of red particles compared to black and white particles [10-12].

Through experiments, it was found that a voltage sequence called driving scheme could control the movement of particles with different colors and charges [13,14], thereby achieving the display of different colors. Therefore, improving the response speed of three-color EPDs by optimizing the driving scheme was of great significance. The traditional driving scheme for a three-color EPD typically involved an erasing stage, an activation stage, and a red driving stage [15-17]. When implementing such a driving scheme for a three-color EPD, the duration required for

ARTICLE IN PRESS

transition from an original image to a target im-age was referred to as the response time. This metric was crucial for assessing the effectiveness of the driving scheme [18-20]. In order to improve the performance of these schemes, an electric field model of EPD was proposed [21-23], providing a theoretical framework for enhancing their overall performance.

By optimizing the driving scheme, some problems of traditional EPDs, such as ex-tended response time, flickering, and ghosting, have been effectively solved [24,25]. For example, an improved reference grayscale driving scheme was proposed [26], which effectively reduced ghosting and was suitable for driving multi-level grayscales. At the same time, a method for shortening response time was proposed [27], but the relationship between particle activity and driving scheme frequency was not analyzed. In addition, a damping oscillation driving scheme was proposed to separate three colored particles in three-color EPDs, which increased the saturation of the red display, but it did not reduce the response time of red particles [28]. Meanwhile, a fast responsive driving scheme was proposed, but the response time of red particles was not further optimized [29]. For three-color EPDs, the volume and mass of red particles are different from black and white particles, which makes it more difficult to drive red color. Therefore, there is still a lot of optimization space for three-color EPDs, such as increasing the saturation of red display and shortening the response time of red particles.

To achieve a rapid response of red particles in three-color EPDs, we proposed a driving scheme on the basis of high-frequency voltage and low-voltage differential oscillation. Analyzing particle movement within microcapsules involved studying Stokes' law and Newton's second law [30,31]. Then, the optimal activation voltage and frequency of the driving scheme were studied to effectively reduce the response time of red particles. At the same time, the implementation of the driving scheme also increased the red saturation, reduced flickering and ghosting phenomena.

2 Principle of Three-Color EPDs

2.1 Preparation materials for three-color EPDs

Electronic ink (E-ink) serves as a pivotal component in the architecture of three-color EPDs, comprising electrophoretic particles, dispersants, charge controllers, and stabilizers. These electrophoretic particles are crucial for displaying images, manifest in three distinct hues: black, white, and red.

Fig. 1 presents the schematic structure of a single pixel in a three-color electrophoretic display. It shows the key components that enable color generation: the black, white, and red pigment particles suspended in a fluid, positioned between a transparent common electrode and a rear pixel electrode. The core operating principle is illustrated by this arrangement;

ARTICLE IN PRESS

by applying specific voltages to the pixel electrode, a vertical electric field is created, selectively moving the positively or negatively charged particles to the top to display either white, black, or red.

Primarily, TiO_2 is chosen as the white electrophoretic particle owing to its remarkable reflectivity and superior optical characteristics. Conversely, carbon black, renowned for its intense pigmentation, serves as the black electrophoretic particle. The red particles are synthesized using diazotized aniline and Naphthol AS. Facilitating the movement of electrophoretic particles within the medium, a non-polar solvent, commonly tetrachloroethylene, was utilized. Polyvinyl alcohol pyrrolidone assumes the role of a charge controller, ensuring the effective charging of electrophoretic particle surfaces. Additionally, stabilizer Span 80 is incorporated to mitigate the aggregation and precipitation of electrophoretic particles.

To mitigate interaction forces and the probability of collisions among electrophoretic particles, a composite coagulation method is adopted, facilitating the dispersion and encapsulation of electronic ink into microcapsules. These microcapsules feature walls are composed of gelatin and arabic gum, preserving optical transparency. The electrode plates within EPDs consist of polyethylene terephthalate-indium tin oxide (PET-ITO) due to its exceptional flexibility. These plates are divided into two sections: a common electrode plate and a pixel electrode plate, with the former being optically transparent. At a microscopic scale, microcapsules with varying shapes and sizes are tightly arranged between the electrode plates, housing particles of three colors. Upon energizing the pixel electrode, a uniform vertical electric field ensues, compelling the particles to distribute uniformly.

Consequently, the macroscopic pixel lattice displays a regular distribution, showcasing images through reflected ambient light using charged particles of varying colors. Notably, the polarity of red and black particles is positive, while white particles exhibit a negative polarity. Thus, by applying a negative voltage to the pixel electrode plate, white particles migrate to the common electrode plate, rendering the pixel white color. Black particles, which have a higher mobility, swiftly reach the top of microcapsule due to the application of a high-amplitude positive voltage, resulting in a black pixel appearance. Conversely, a low-amplitude positive voltage drives red particles to the common electrode plate, eliciting a red pixel appearance. This voltage regulation mechanism governs particle motion states, effectuating changes in pixel color.

ARTICLE IN PRESS

ARTICLE IN PRESS

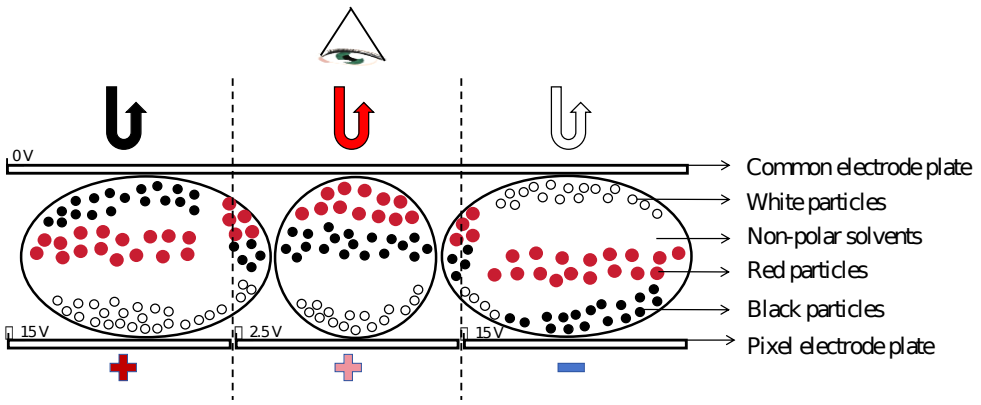

Fig. 1. Pixel structure schematic diagram of three-color EPDs. Each pixel comprises black, white and red particles suspended in non-polar solvents, along with a pixel electrode plate and a common electrode plate.

2.2 The driving principle of three-color EPDs

Electrophoretic particles are controlled by the driving scheme, which affects the display quality of EPDs. Therefore, analyzing the motion state of electrophoretic particles is of great significance. Throughout the driving process in EPDs, particles experience a blend of viscosity and electrostatic force. The interplay between viscosity and electrostatic force can be deduced from electrophoresis theory and Stokes' theorem, as shown in equation (1).

$$F = ma = m\frac{\Delta v}{\Delta t} = \frac{qU}{d} - 6\pi\eta Rv \quad (1)$$

Among these variables, F represents the combined force exerted on electrophoretic particles within the system. m denotes the mass of the particle, a signifies its acceleration, v embodies the particle's velocity, and R encapsulates its radius. Additionally, t delineates the duration of voltage application across the electrode plates of EPDs, while U characterizes the real-time voltage applied to an individual pixel. q quantifies the charge magnitude carried by each particle, d stands for the spatial separation between the two EPD electrode plates. η symbolizes liquid's viscosity coefficient, which is a crucial factor influencing particle movement. Once the voltage is introduced, the motion of particles can be described by a velocity equation, succinctly expressed by equation (2).

ARTICLE IN PRESS

$$v = \frac{Uq}{6\pi d\eta R}\left(1 - e^{-\frac{6\pi\eta R t}{m}}\right) \quad (2)$$

By integrating the particle velocity, the relationship between the particle motion distance □ and the applied voltage time □$_s$ can be obtained, as

$$□ = \int_0^{t_s} v\,dt = \frac{Uq}{6\pi d\eta R}\left(t + \frac{m e^{-\frac{6\pi\eta R t_s}{m}}}{6\pi\eta R}\right) - \frac{Uqm}{36\pi^2\eta^2 R^2 d} \quad (3)$$

expressed in equation (3).

Where □ is the motion distance of particles, □ is directly proportional to □$_s$. In equation (3), it can be seen that the shorter the driving voltage time, the smaller the distance of particles' movement. Hence, upon the application of high-frequency voltage, particles oscillate within a specific range, and this range diminishes as the frequency rises. Yet, excessively high frequencies limit particle movement due to their reduced oscillation distance. Conversely, an optimal level of high-frequency voltage permits particles to oscillate within a confined range, thereby enhancing particle activity more effectively.

2.3 Simulation model of three-color EPDs

In order to study the impact of the high-frequency voltage and low-voltage differential oscillation on particles, we utilized COMSOL to construct a three-color EPD particle motion model. In this model, pixel electrode plates, microcapsules, and a common electrode plate formed a stacked structure, As shown in Fig. 2 (a). At the same time, the coupling of a laminar flow field, a fluid flow particle tracking field, and an electrostatic field were added to the model. The laminar flow field is a simulation method suitable for low velocity liquid. The electrostatic field provided an electrostatic field for driving three-color EPDs. The fluid flow particle tracking field is a simulation method for tracking motion changes of particles at the interface.

$$F_t = \frac{d}{dt}\left(m_p \frac{dr}{dt}\right) \quad (4)$$

When particles move in a fluid, they follow Newton's second law of motion, as expressed in equation (4).

Among them, m_p represents the mass of the particle, r represents the position vector of the particle, and F_t signifies the net or total force acting upon the particle. For a particle sinking in a fluid, the total force F_t encompasses both gravity F_g and drag F_D, as articulated by equation (5) and (6).

ARTICLE IN PRESS

$$F_g = \frac{\rho_p - \rho}{\rho_p} m_p g \quad (5)$$

$$F_D = 3\pi\mu d_p(u - v) \quad (6)$$

Among them, ρ_p represents the density of particles, ρ represents the density of the encompassing fluid, g represents the acceleration due to gravity (approximately 9.8 m/s^2 below sea level), μ represents the dynamic viscosity of the surrounding fluid, d_p represents the particle size, u represents the velocity of the surrounding fluid, and v represents the velocity of particles.

In the simulation model, when particles and the surrounding fluid had the same density, their buoyancy value approached zero. In this case, particles were called suspended particles. Combining equations (4)-(6), we obtained a simplified expression for the particle motion equation, as expressed in equation (7).

$$\frac{d^2r}{dt^2} = \frac{\rho_p - \rho}{\rho_p} g + \frac{1}{\tau_p}(u - v) \quad (7)$$

$$\tau_p = \frac{\rho_p {d_p}^2}{18\mu} \quad (8)$$

The constant τ_p was introduced in equation (7), as shown in equation (8). τ_p had a time unit and was commonly referred to as the Lagrangian time scale or particle velocity response time, which had a significant impact on the simulation results.

The application of square wave voltages with different frequencies and amplitudes could alter particles' motion state. As shown in Fig. 2 (b) and 2 (c), we presented a schematic diagram of the vertical motion trajectory of three-color particles. Under conditions of a high-frequency voltage of 100 Hz and a low-voltage differential oscillation voltage of 5 V, red particles were activated quickly and moved towards the common electrode plate. At this time, black particles were not effectively activated, it could provide a good red display in this situation. Based on these simulation results, it was found that the introduction of high-frequency voltage and low-voltage differential oscillation voltage could improve the response speed of red particles, and further increase their motion distance. So, we designed a driving scheme based on simulation results for achieving an ideal red display.

ARTICLE IN PRESS

ARTICLE IN PRESS

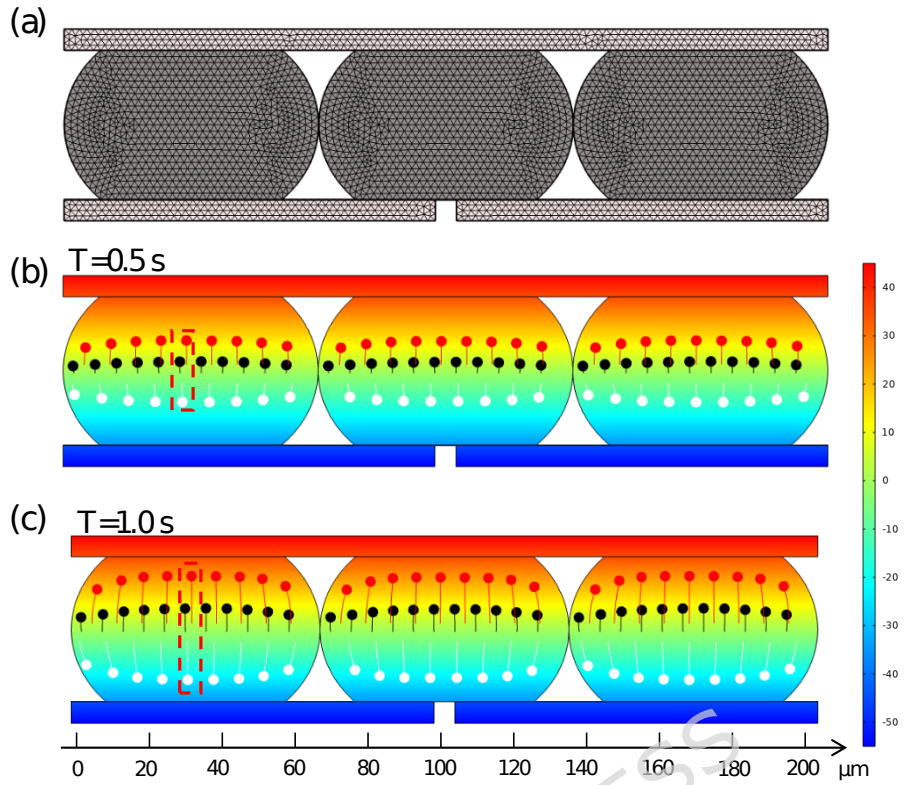

Fig. 2. Three-color EPD simulation model diagram (a) The three-color EPD model established by COMSOL. (b) Schematic diagram of vertical motion trajectory of three-color particles at 0.5 s. (c) Schematic diagram of vertical motion trajectory of three-color particles at 1.0 s.

3 Experimental Results and Discussion

3.1 Experimental Platform

To evaluate the efficacy of driving schemes, we devised an optical experimental setup illustrated in Fig. 3. This experimental configuration facilitated the assessment of brightness levels and red saturation in three-color EPDs during red display states, and could also characterize the response time of red particles based on red saturation. The experimental apparatus comprised a computer (H430, Lenovo, Beijing, China), a function generator (AFG3022C, Tektronix, Beaverton, OR, USA), a signal amplifier (ATA-2022H, Agitek, Xi'an, China), an EPD driver panel and a colorimeter (Arges-45, Admesy, Itervoort, The Netherlands).

ARTICLE IN PRESS

In a complete process of the experiment, MATLAB and Arbexpress software were first used to edit the driving scheme and generate a file as TIFF World File (TFW), which could be recognized by the function generator. Next, we transfered the compiled driver scheme file to the function generator via Universal Serial Bus (USB). Then, a signal amplifier was used to increase the voltage and connect positive and negative electrodes of the EPD driver panel to display different colors. Finally, we placed the colorimeter directly above the three-color EPD, equipped with a constant light source. To ensure accurate measurement, we calibrated the colorimeter regularly using standard color reference samples and recorded the brightness and red saturation of the three color EPD in real time using Admesi software. The brightness value was the brightness reflected by the three-color EPD, and the red saturation referred to the purity of the red color displayed by the three-color EPD.

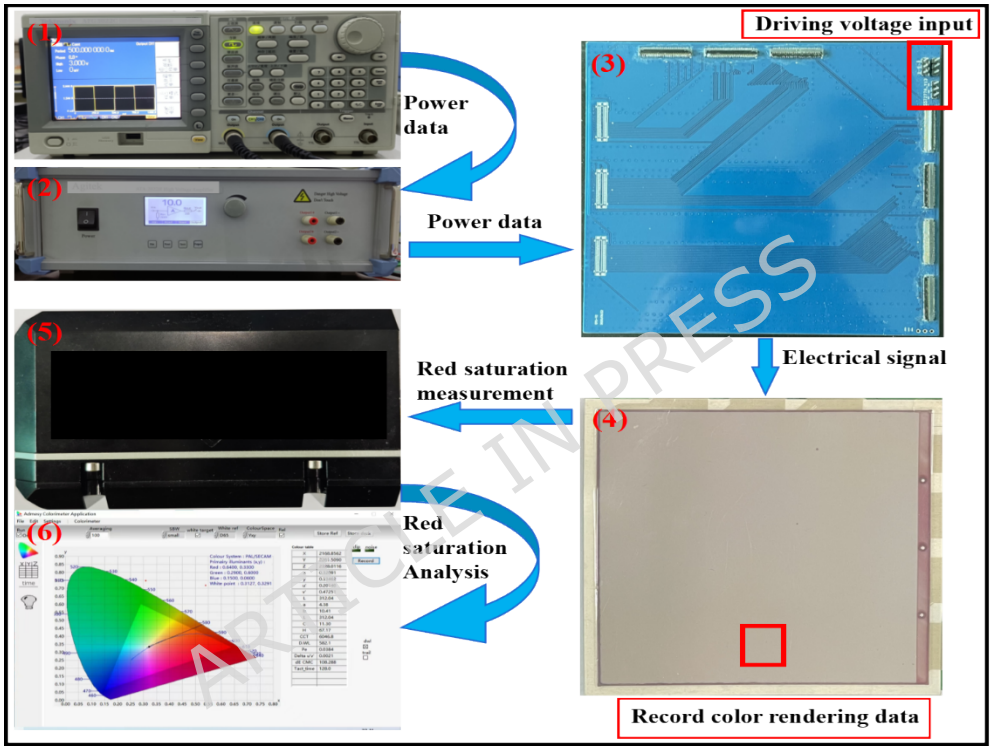

Fig. 3. Experimental platform for testing the performance of EPDs. It consisted of a driving system and a testing system. (1) Function generator (2) Signal amplifier (3) EPD Driver Panel (4) Three-color electrophoretic display (5) Colorimeter (6) Computer.

ARTICLE IN PRESS

3.2 Driving scheme design

In this paper, based on the simulation results, a new driving scheme was proposed and validated, which achieved the goal of reducing response time and increasing red saturation by using high-frequency voltage and low-voltage differential oscillation scheme. As shown in Fig. 4, -15 V was set as the driving voltage in the erasing stage, which could drive the three-color EPD to a uniform gray level. By adjusting activation voltages V_{A1}, V_{A2} and their driving times T_{A2}, T_{A3}, red particles could be activated during the activation stage, during which they continuously moved up and down through high-frequency oscillation voltage to obtain initial kinetic energy, preparing adequately for the driving stage. Meanwhile, the erasing stage time T_{E2} and the red driving stage time T_{R2} were tested under the condition of satisfying the direct current (DC) balance rule, which means that the net DC voltage established at both ends of the EPD unit was close to zero. Without following the DC equilibrium rule, the electrochemical characteristics of particles drifting inside the electrophoretic material might change. This increased the risk of irreversible damage to the entire EPD, these parameters were given by equation (9).

$$-15V \times T_{E2} + V_R \times T_{R2} = 0 \tag{9}$$

Among them, T_{E2} was the time of the erasing stage, V_R and T_{R2} represented the voltage and time of the red driving stage, respectively.

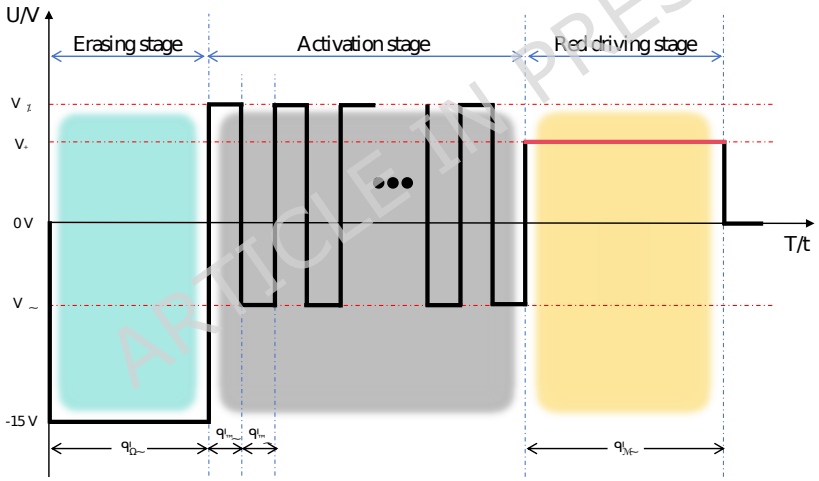

Fig. 4. The driving scheme proposed in this paper consisted of an erasing stage, an activation stage and a red driving stage. The time of the erasing stage was T_{E2}, T_{A2} was the time of positive voltage during the oscillation period, and T_{A3} was the time of negative voltage during the oscillation period. The red driving time was T_{R2}. Positive and negative voltage values during the activation phase were V_{A1} and V_{A2}, respectively.

ARTICLE IN PRESS

3.3 Parameter optimization of driving scheme

For the proposed driving scheme, all parameters need to be optimized. Firstly, adjustments were made to the driving voltage V_R and driving time T_{R2} during the display of red, followed by testing the red saturation. The value of T_{E2} was set to 500 ms, and the range of V_R was set from 1 V to 5 V. As V_R changed, the change of red saturation was shown in Fig. 5 (a). Error bar was obtained from five repeated experiments. These results indicated that as V_R increased from 1 V to 2.5 V, there was a positive correlation between red saturation and V_R. Consequently, when the positive voltage remained below the threshold voltage of red particles, red particles failed to migrate to the common electrode, resulting in low red saturation. When V_R increased from 2.5 V, there was a negative correlation between the red saturation and V_R. This occurs because exceeding the threshold voltage of black particles leaded to the simultaneous migration of black and red particles to the common electrode, resulting in a mixed black and red coloration and a subsequent reduction in red saturation. When V_R was set to 2.5 V, red particles could be driven to the maximum extent, and the red saturation could reach 0.42.

Fig. 5(b) illustrated the variation of the red saturation with T_{R2}, and the error bars represented the standard deviation derived from five repeated experiments. Throughout these experiments, V_R remained constant at 2.5 V, while T_{R2} values ranged from 2000 ms to 4000 ms. Notably, an observable trend emerged as the duration of driving increased. As the driving time increased, it gradually reached a peak of 0.45 in red saturation. However, as the driving duration prolonged, red saturation tended to plateau, indicating saturation. Consequently, the optimal T_{R2} was determined to be 3000 ms.

To determine the optimal activation voltage for red particles, we investigated the effects of various V_{A1}s and V_{A2}s values. To maintain DC balance, V_{A1}s and V_{A2}s were set to opposite polarity voltages, with their difference representing the amplitude of the oscillation voltage. The activation stage's oscillation period was fixed at 10 ms, with 30 oscillations in total. Fig. 5 (c) displays the red saturation corresponding to different oscillation voltage amplitudes. We observed that red saturation increased as the voltage amplitude rose from 2 V to 6 V, but decreased beyond 6 V. Consequently, red particle activity augmented with increasing voltage amplitude below 6 V, whereas above 6 V, black particle activity intensified, diminishing red saturation. Therefore, setting the oscillation voltage amplitude to 6V yielded the optimal activation voltage for red particles.

In refining the proposed driving scheme, the frequency of the high-frequency oscillation voltage played a pivotal role. Insufficient frequency led to noticeable flickering, while excessively high frequency resulted in short cycle times, limiting particle activity due to their restricted oscillation

ARTICLE IN PRESS

range as equation (3). We explored five oscillation periods (10 ms, 15 ms, 20 ms, 25 ms, and 30 ms) and four number of oscillation times (10, 20, 30, and 40), recording the red saturation for each combination. Fig. 5(d) illustrates that red saturation increased with decreasing oscillation period and increased with increasing oscillation times. The optimal red saturation of 0.5302 was achieved with an oscillation period of 10 ms and 30 oscillations. This indicates that red particles could be activated without activating black and white particles through high-frequency, low-voltage oscillation. However, while increasing frequency and oscillations enhanced red saturation, excessive oscillations extended the response time. Consequently, in the proposed driving scheme, the oscillation period was set at 10 ms with 30 oscillations.

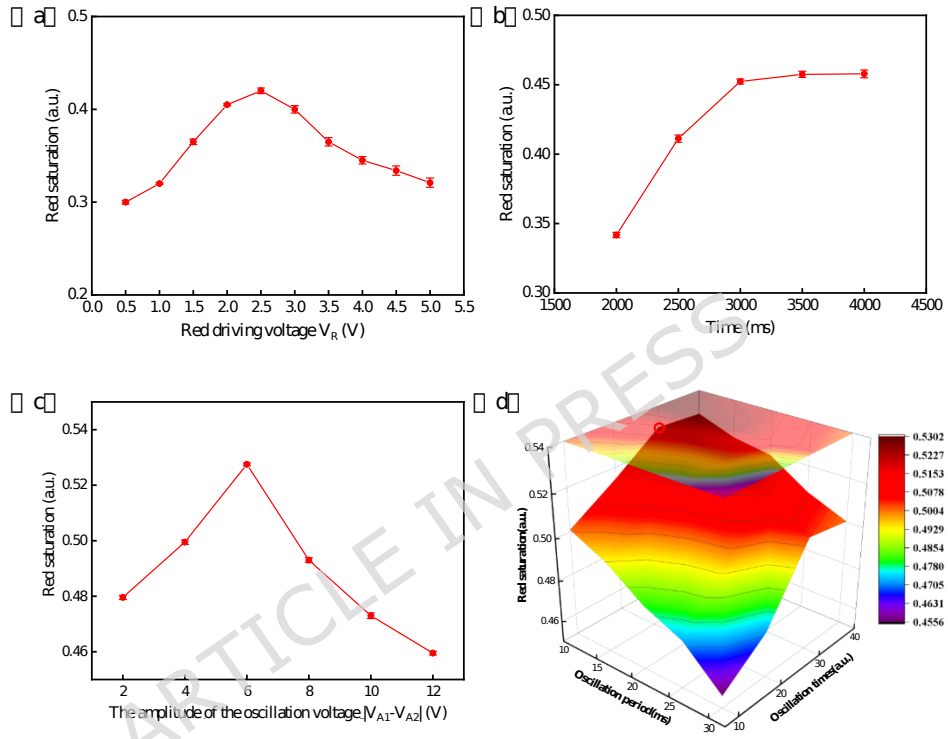

Fig. 5. Red saturation variation chart. (a)When a traditional driving scheme was used to drive a three-color EPD, the red saturation changed with the change of V_R. (b) When a traditional driving scheme was used to drive a three-color EPD, red saturation changed with the change of T_{R1}. (c) When the amplitude of the oscillation voltage $|V_{A1} - V_{A2}|$ was low, red particles could not be effectively activated. When the amplitude of the oscillation voltage $|V_{A1} - V_{A2}|$ was high, black particles were also driven to the common electrode plate. (d) Influence of oscillation period and oscillation times on red saturation.

ARTICLE IN PRESS

3.4 Display performance comparison of driving schemes

When the target color of the three-color EPD was red, the traditional driving scheme and the driving scheme with photometric calibration were shown in Fig. 6 (a) [16,19]. Both driving schemes consisted of three stages: erasing stage, activation stage, and a target color driving stage. As illustrated in Fig. 6 (b), by adjusting the driving time and amplitudes, charged particles of different colors were driven to different positions inside the microcapsule, thereby achieving display of different colors. To display red, the three-color EPD wasted a long time in erasing and activation stages of these two driving schemes, thereby prolonging the response time of red particles. In addition, the square wave frequency used during the activation stage was too low, alternating between positive and negative voltages could cause significant flickering phenomena.

Subsequently, the maximum red saturation achieved by the proposed driving scheme was compared with that of the other two schemes. The grayscale conversion process for each stage is illustrated in Fig. 6 (c). The first column depicts the traditional driving process, the second column shows the process with photometric calibration, and the third column displays the proposed scheme. It is evident that the proposed scheme employs high-frequency voltage and low-voltage differential oscillation to activate and separate red particles. During the activation stage, red particles were effectively activated and the EPD appeared light red, ultimately achieving better red display than the other two driving schemes.

ARTICLE IN PRESS

ARTICLE IN PRESS

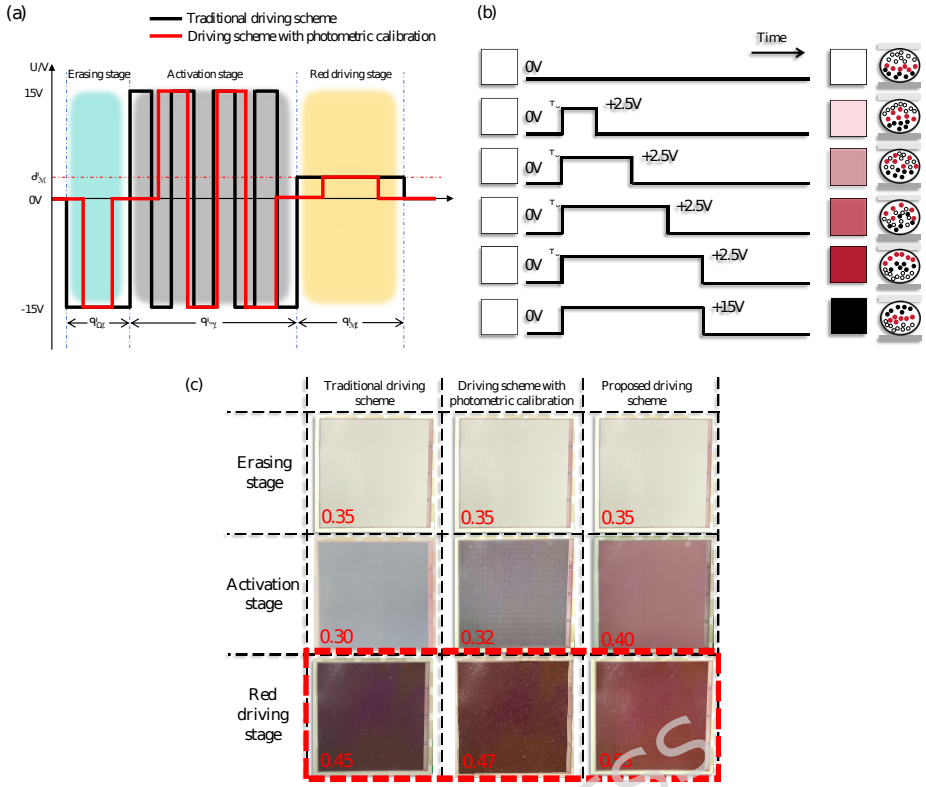

Fig. 6. Comparative experimental diagram for measuring red saturation. (a) Traditional driving scheme and Driving scheme with photometric calibration of the three-color EPD (b) PWM driving scheme diagram. (c) Display image conversion of three-color EPD under different driving schemes.

Meanwhile, the performance was compared with the other two driving schemes based on brightness flickers and red particle response time, as shown in Fig. 7 [29,32]. As shown in Fig. 7 (a), the five color curves represented the process of luminance change when applying the five driving schemes. In Fig. 7 (b), the flicker phenomenon during the activation stage of the traditional driving scheme was shown. In Fig. 7 (c), the flicker phenomenon during the activation stage of the driving scheme with photometric calibration was shown. Corresponding serial number annotations were used in Fig. 7 (a), (b), and (c), It could be seen that there will be serious flickering phenomenon, leading to poor display effect. In Fig. 7 (d), the five color curves were also used to represent changes in red saturation of three-color EPDs under different driving schemes. The comparison of display performance parameters for five driving schemes was shown in Table 1. Experimental results showed that, compared to the other four driving schemes, the proposed driving scheme reduced the

ARTICLE IN PRESS

response time of red particles by 2.42 s, decreased the number of flickers by 8 times, and the red saturation was increased by 0.08.

Table 1 Comparison of display performance parameters for five driving schemes

Driving schemes	Response time	Maximum red saturation	Number of flickers
Driving scheme with photometric calibration [19]	3.58 s	0.47	5
Speed driving scheme [29]	2.28 s	0.51	3
Traditional driving scheme [16]	4.18 s	0.45	9
Fast response driving scheme [32]	2.31 s	0.52	3
Proposed driving scheme	1.76 s	0.53	1

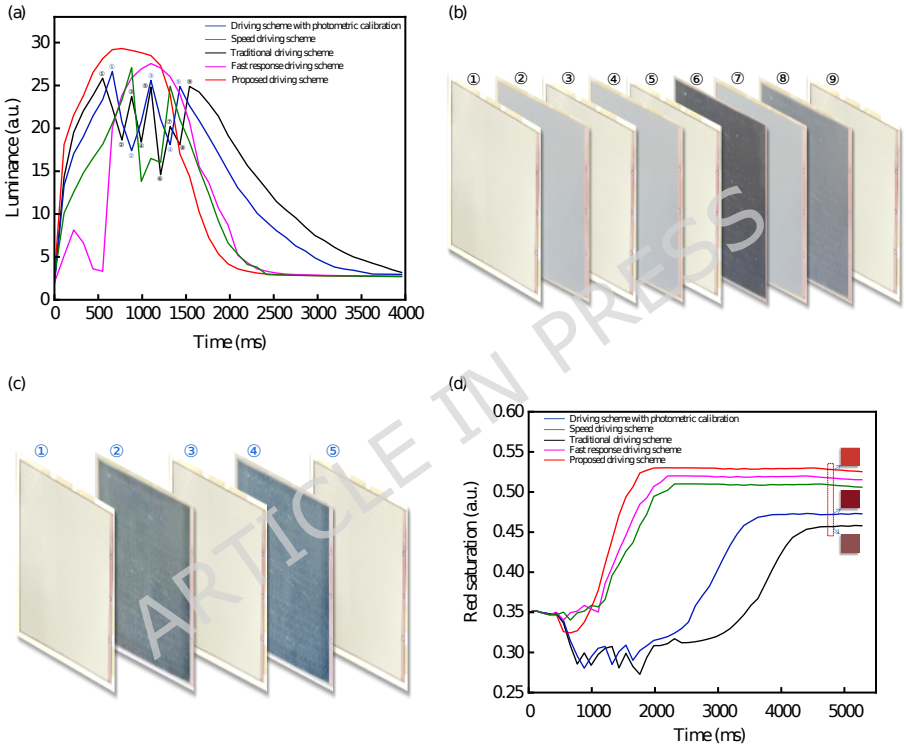

Fig. 7. The performance of the three-color EPD by applying five different driving schemes. (a) The change process of luminance. (b) Flicker process diagram of the traditional driving scheme. (c) Flicker process diagram of the driving scheme with photometric calibration. (d) The change process of red saturation.

ARTICLE IN PRESS

4 Conclusions

In this paper, we proposed a new driving scheme based on high-frequency voltage and low-voltage differential oscillation for improving the performance of three-color EPDs. Due to the low-voltage oscillation scheme, red particles were effectively activated, which increased the red saturation and shortened the response time of red particles. The high-frequency voltage during the activation stage effectively solved the problem of flickers, thereby improving the display performance of images. Compared with other driving schemes, the proposed driving scheme could effectively reduce response time and flickers, and increase red saturation. So, our proposed driving scheme could provide certain reference values for three-color EPD applications and development.

Author Contributions: M.J. designed this project and conducted most experiments and data analysis. Z.Y. performed part of the experiments and helped with discussions during manuscript preparation. L.L. and F.C. revised the paper. J.W., W.X. and Z.L. gave suggestions on project management. L.W. and G.Z. provided helpful discussions on the experimental results. All authors have read and agreed to the published version of the manuscript.

Funding: This work was supported by the National Natural Science Foundation of China (no. 62105056), the Special Project in Key Fields of Regular Universities in Guangdong Province (no. 2022ZDZX1046), the Guangdong Provincial Key Laboratory of Optical Information Materials and Technology(no. 2023B1212060065), the Engineering Technology Center of Regular Universities in Guangdong Province (no. 2021GCZX005), the Innovation Team of Regular Universities in Guangdong Province (no. 2021KCXTD040), the Key Laboratory of Regular Universities in Guangdong Province (no. 2023KSYS011).

Data Availability Statement: Data is contained within the article.

Conflicts of Interest: The authors declare no conflict of interest.

ARTICLE IN PRESS

References

[1] T. Bert and H. De Smet, The microscopic physics of electronic paper revealed. Displays. 24, 103-110 (2003).

[2] J. Cao, Z. Qin, Z. Zeng, W. Hu, L. Song, D. Hu, X. Wang, X. Zeng, Y. Chen and B. Yang, A convolutional neural network for ghost image recognition and waveform design of electrophoretic displays. IEEE Transactions on Consumer Electronics. 66, 356-365 (2020).

ARTICLE IN PRESS

[3] F. Duan, P. Bai, A. Henzen, L. Shui, B. Tang and G. Zhou, An adaptive generation method for electrophoretic display driving waveform design. Journal of the Society for Information Display. 24, 676-685 (2016).

[4] C. Gu, A. Jia, Y. Zhang and S. X. A. Zhang, Emerging electrochromic materials and devices for future displays. Chemical Reviews. 122, 14679-14721 (2022).

[5] W. He, Z. Yi, S. Shen, Z. Huang, L. Liu, T. Zhang, W. Li, L. Wang, L. Shui and C. Zhang, Driving waveform design of electrophoretic display based on optimized particle activation for a rapid response speed. Micromachines. 11, 498 (2020).

[6] J. Heikenfeld, P. Drzaic, J. S. Yeo and T. Koch, A critical review of the present and future prospects for electronic paper. Journal of the Society for Information Display. 19, 129-156 (2011).

[7] M. Jin, S. Shen, Z. Yi, G. Zhou and L. Shui, Optofluid-based reflective displays. Micromachines. 9, 159 (2018).

[8] M. T. Johnson, G. Zhou, R. Zehner, K. Amundson, A. Henzen and J. Van De Kamer, High-quality images on electrophoretic displays. Journal of the Society for Information Display. 14, 175-180 (2006).

[9] W. C. Kao, H. Y. Chen, Y. H. Liu and S. C. Liou, Hardware engine for supporting gray-tone paintbrush function on electrophoretic papers. Journal of Display Technology. 10, 138-145 (2013).

[10] W. C. Kao and J. C. Tsai, Driving method of three-particle electrophoretic displays. IEEE Transactions on Electron Devices. 65, 1023-1028 (2018).

[11] W. C. Kao, J. A. Ye, F. Lin, P. Cheng and R. Sprague, Configurable timing controller design for active matrix electrophoretic display. IEEE Transactions on Consumer Electronics. 55, 1-5 (2009).

[12] M. K. Kim, Y. J. Lim, S. S. Bhattacharyya, M. H. Lee and S. H. Lee, Control of motion of fullerene colloidals by dielectrophoretic force for electronic paper-like display. Current Applied Physics. 11, 1192-1196 (2011).

[13] Y. C. Kim, An Analysis of Reflectivity and Response Time by Charge-to-Mass of Charged Particles in an Electrophoretic Display.

ARTICLE IN PRESS

Transactions on Electrical and Electronic Materials. 17, 212-216 (2016).

[14] J. K. Lee, S. S. Kim, Y. I. Park, C. D. Kim and Y. K. Hwang, In-cell adaptive touch technology for a flexible e-paper display. solid-state electronics. 56, 159-162 (2011).

[15] W. Li, L. Wang, T. Zhang, S. Lai, L. Liu, W. He, G. Zhou and Z. Yi, Driving waveform design with rising gradient and sawtooth wave of electrowetting displays for ultra-low power consumption. Micromachines. 11, 145 (2020).

[16] Y. Liu, Q. Fan, G. Liu, Z. Li, J. Liu, J. Yang, T. Zhou, Z. Zeng, Z. Qin and B.-R. Yang, Active matrix driven electrophoretic display with in-plane switching layout and driving waveform for reflective and transparent modes. Optics Express. 31, 40102-40112 (2023).

[17] C. M. Lu and C. L. Wey, A controller design for high-quality images on microcapsule active-matrix electrophoretic displays. Journal of Information Display. 13, 21-30 (2012).

[18] Z. Qin, H. I. Wang, Z. Y. Chen, C. H. Chen, P. L. Tien, M. H. Liu, S. C. Liu, C. M. Hung, C. C. Tsai and Y. P. Huang, Digital halftoning method with simultaneously optimized perceptual image quality and drive current for multi-tonal electrophoretic displays. Applied Optics. 59, 201-209 (2020).

[19] S. Shen, Y. Gong, M. Jin, Z. Yan, C. Xu, Z. Yi, G. Zhou and L. Shui, Improving electrophoretic particle motion control in electrophoretic displays by eliminating the fringing effect via driving waveform design. Micromachines. 9, 143 (2018).

[20] L. Wang, Z. Yi, B. Peng and G. Zhou, In AOPC 2015: Advanced Display Technology; and Micro/Nano Optical Imaging Technologies and Applications, (SPIE: 2015), pp 14-22.

[21] W. Xu, Z. Yi, M. Jiang, J. Wang, Z. Long, L. Liu, F. Chi, L. Wang and Q. Wan, High-Performance Multi-Level Grayscale Conversion by Driving Waveform Optimization in Electrowetting Displays. Micromachines. 15, 137 (2024).

[22] S. H. Yang, F. C. Lin, Y. P. Huang, H. P. Shieh, B. R. Yang, M. J. Chang, J. C. Huang and Y. J. Hsieh, In SID Symposium Digest of Technical Papers, (Wiley Online Library: 2012), pp 1361-1364.

ARTICLE IN PRESS

ARTICLE IN PRESS

[23] Z. Yi, P. Bai, L. Wang, X. Zhang and G. Zhou, An electrophoretic display driving waveform based on improvement of activation pattern. journal of central south university. 21, 3133-3137 (2014).

[24] Z. Yi, H. Feng, X. Zhou and L. Shui, Design of an open electrowetting on dielectric device based on printed circuit board by using a parafilm m. Frontiers in Physics. 8, 193 (2020).

[25] Z. Yi, L. Shui, L. Wang, M. Jin, R. A. Hayes and G. Zhou, A novel driver for active matrix electrowetting displays. Displays. 37, 86-93 (2015).

[26] Z. Yi, W. Zeng, S. Ma, H. Feng, W. Zeng, S. Shen, L. Shui, G. Zhou and C. Zhang, Design of driving waveform based on a damping oscillation for optimizing red saturation in three-color electrophoretic displays. Micromachines. 12, 162 (2021).

[27] D. Yu, J. An, J. Bae, D. Jung, S. Kim, S. Ahn, S. Kang and K. Suh, Preparation and characterization of acrylic-based electronic inks by in situ emulsifier-free emulsion polymerization for electrophoretic displays. Chemistry of materials. 16, 4693-4698 (2004).

[28] W. Zeng, Z. Yi, Y. Zhao, W. Zeng, S. Ma, X. Zhou, H. Feng, L. Liu, L. Shui and C. Zhang, Design of driving waveform based on overdriving voltage for shortening response time in electrowetting displays. Frontiers in Physics. 9, 642682 (2021).

[29] W. Zeng, Z. Yi, X. Zhou, Y. Zhao, H. Feng, J. Yang, L. Liu, F. Chi, C. Zhang and G. Zhou, Design of driving waveform for shortening red particles response time in three-color electrophoretic displays. Micromachines. 12, 578 (2021).

[30] H. Zhang, Z. Yi, S. Ma, S. Deng, W. Zhou, W. Zeng, L. Liu, F. Chi, Y. Hu and C. Zhang, Design of Driving Waveform for Shortening Response Time of Black Particles and White Particles in Three-Color Electrophoretic Displays. Micromachines. 12, 1306 (2021).

[31] Y. Zhang, B. Zhen, S. A. S. Al-Shuja'a, G. Zhou, X. Li and Y. Feng, Fast-response and monodisperse silica nanoparticles modified with ionic liquid towards electrophoretic displays. Dyes and Pigments. 148, 270-275 (2018).

[32] Y. Zhang, B. Zhen, R. Li, S. Meng, X. Li and Y. Feng, Low density and fast response silica coated with ionic liquid polymer nanoparticles

ARTICLE IN PRESS

towards electrophoretic displays. Materials Letters. 211, 17-20 (2018).

ARTICLE IN PRESS